Impact of Airfoils on Aerodynamic Optimization of Heavy Lift Rotorcraft

C. W. Acree, Jr.
Aerospace Engineer
NASA Ames Research Center
Moffett Field, CA
cecil.w.acree@nasa.gov

Preston B. Martin
Research Scientist
Aeroflightdynamics Directorate (AMRDEC)
Moffett Field, CA
pmartin@merlin.arc.nasa.gov

Ethan A. Romander
Aerospace Engineer
NASA Ames Research Center
Moffett Field, CA
eromander@mail.arc.nasa.gov

Abstract

Rotor airfoils were developed for two large tiltrotor designs, the Large Civil Tilt Rotor (LCTR) and the Military Heavy Tilt Rotor (MHTR). The LCTR was the most promising of several rotorcraft concepts produced by the NASA Heavy Lift Rotorcraft Systems Investigation. It was designed to carry 120 passengers for 1200 nm, with performance of 350 knots cruise at 30,000 ft altitude. A parallel design, the MHTR, had a notional mission of 40,000 lb payload, 500 nm range, and 300 knots cruise at 4000 ft, 95 F. Both aircraft were sized by the RC code developed by the U. S. Army Aeroflightdynamics Directorate (AFDD). The rotors were then optimized using the CAMRAD II comprehensive analysis code. Rotor airfoils were designed for each aircraft, and their effects on performance analyzed by CAMRAD II. Airfoil design criteria are discussed for each rotor. Twist and taper optimization are presented in detail for each rotor, with discussions of performance improvements provided by the new airfoils, compared to current technology airfoils. Effects of stall delay and blade flexibility on performance are also included.

Notation

A	rotor disk area
C_l	section lift coefficient
C_m	section pitching moment coefficient
C_T	rotor thrust coefficient, $T/(\rho A V^2_{tip})$
D	drag
F_c	fuel consumed
L	lift
M	figure of merit; Mach number
q	dynamic pressure
R	rotor radius
Re	Reynolds number
t/c	thickness to chord ratio
T	rotor thrust
V_{tip}	rotor tip speed
α	angle of attack
η	propulsive efficiency
ρ	air density
σ	rotor solidity (ratio blade area to disk area)
ISA	international standard atmosphere
LCTR	Large Civil Tilt Rotor
MHTR	Military Heavy Tilt Rotor
OEI	one engine inoperative
SFC	specific fuel consumption
SOA	state of the art

Presented at the AHS Vertical Lift Aircraft Design Conference, San Francisco, California, January 18-20, 2006.

Introduction

A new generation of very large, fast rotorcraft is being studied to meet emerging transportation requirements. With gross weights in excess of 100,000 lb and speeds of 300 knots or greater, such aircraft will face severe aerodynamic design challenges to meet acceptable efficiency. This paper addresses the aerodynamic optimization of rotors for such aircraft, with special attention to the impact of new airfoils on tiltrotor performance.

NASA recently completed the Heavy Lift Rotorcraft Systems Investigation (Ref. 1), which studied several design concepts for high-speed rotorcraft. The Large Civil Tiltrotor (LCTR) proved to be the preferred concept and is given close attention here. The Large Civil Tandem Compound (LCTC) also looked promising; its design optimization is discussed in Ref. 2.

A parallel effort studied the Military Heavy Tiltrotor (MHTR). Although given less emphasis than the civil designs, the MHTR study generated results that make for instructive comparisons with the LCTR. This paper focuses on aerodynamic design and optimization of the LCTR and MHTR rotors.

This paper begins with a summary of aircraft design requirements for the two vehicles. The iterative rotor design process is summarized, then the airfoil design requirements are briefly discussed. Twist and taper optimization are discussed in detail and are used to illustrate the effects of airfoils, stall delay, and blade flexibility on performance. The MHTR rotor optimization is discussed first to illustrate the design approach. Discussion of the more challenging LCTR design follows and concludes the paper.

Tiltrotor Conceptual Designs

Tables 1 and 2 summarize the mission requirements for the two aircraft. The objective of the LCTR design is to be competitive with regional jets and compatible with future, crowded airspace. The baseline civil mission is defined by NASA technology goals (Ref. 1). The military mission is based on numerous studies by the Aviation Advanced Design Office of the U. S. Army Aeroflightdynamics Directorate (AFDD), RDECOM. The MHTR mission is purely notional and provides an instructive contrast with the civil mission.

Table 1. NASA civil heavy-lift mission.

Payload	120 passengers = 26,400 lb (with baggage)
Range	1200 nm
Cruise	Mach 0.6 at 30,000 ft (350 kts)
Hover at Denver	5,000 ft ISA + 20C (OEI at 22K ISA)
All weather operations	CATIIIC SNI
Community noise	SOA –14 EPNdb

Table 2. MHTR notional mission requirements.

Payload	40,000 lb, 11x9x40 ft (modified C-130 cargo box)
Range	500 nm (2x250 nm)
Hover	OEI at 4000 ft, 95F (4K/95)
Cruise	Best productivity speed at 4K/95 (300 knots desired)
Shipboard compatible	Max width 167.5 ft

Figure 1 summarizes the iterative process that produced the concept designs from the mission requirements. The rotorcraft design software RC performed the sizing of the rotorcraft, including mission performance analysis (Ref. 3). The software package CAMRAD II was used for rotor performance optimization and for loads and stability calculations. CAMRAD II performs aeromechanical analysis for rotorcraft, utilizing a combination of advanced technologies, including multibody dynamics, nonlinear finite elements, and rotorcraft aerodynamics (Ref. 4). Other codes, including NASTRAN and HeliFoil, were used for subsystem analyses. Reference 1 discusses the integration of the various design tools and methodologies into an global design process.

The design process accommodated design requirements in addition to the basic mission specifications. For example, rotor tip speed was set by noise requirements in hover (LCTR) and efficiency requirements in cruise. The RC design code then determined the rotor radius and solidity required to meet the mission requirements in Tables 1 and 2; the entire aircraft was sized simultaneously with the rotor. Rotor performance capability was derived by RC from scaling rules and technology factors. For example, drag was scaled from historical trends, with an additional factor representing new technology.

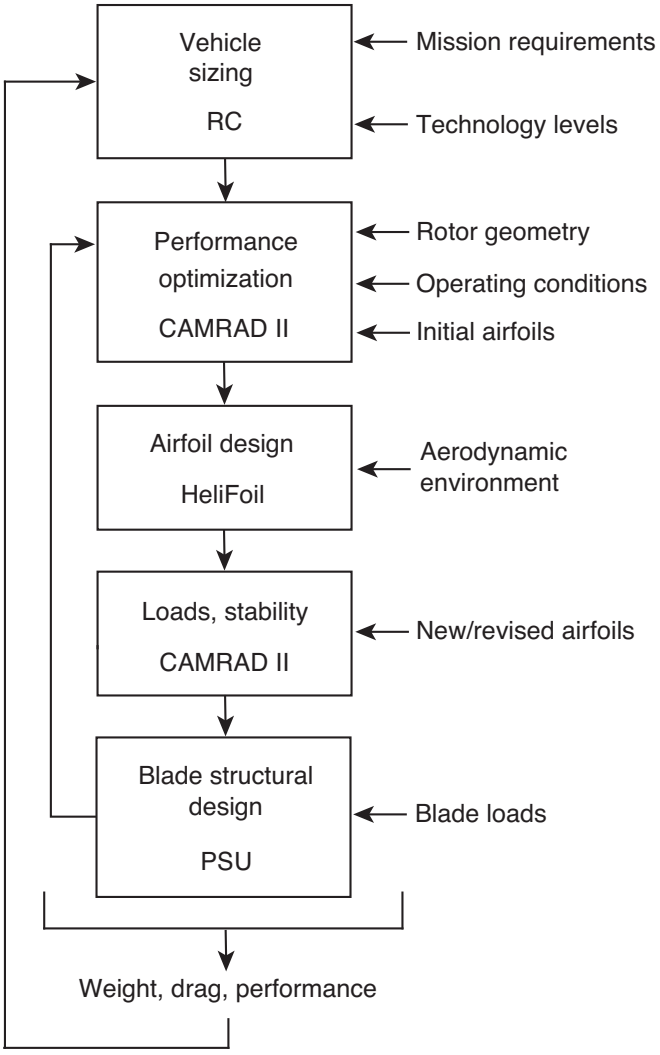

Fig. 1. Iterative rotor design process.

The notional rotor defined by RC was then aerodynamically optimized by CAMRAD II, using current technology (SOA) airfoils (Ref. 5). Twist and taper were determined by selecting the optimum performance values from a large matrix of CAMRAD II analyses that covered both cruise and hover. The blade structural design was developed by Pennsylvania State University (PSU) to meet the loads calculated by CAMRAD II; see Ref. 6 for details of the blade structural design procedure. If needed, the rotor was reoptimized without resizing the aircraft (inner loop of Fig. 1). To begin another optimization cycle, RC was

recalibrated to match the detailed CAMRAD II predictions for the current design.

There was an option to add new, purpose-designed airfoils after initial optimization. The airfoil design was driven by the local flow conditions computed earlier in the optimization cycle. This typically required another cycle of rotor optimization (inner loop) to maximize the benefits of new airfoils.

Table 3 summarizes the resulting design values for the two concepts, which are illustrated in Figs. 2 and 3. The LCTR is designed for 350 knots at 30,000 ft altitude, with low disk loading in hover. It has a low cruise tip speed of 350 ft/sec for high efficiency and a hover tip speed of 650 ft/sec for low noise. The MHTR is designed for 300 knots at 4000 ft altitude (95 F), with higher disk loading and tip speeds. The two designs are within 6% of gross weight, but the rotor optimization yielded significantly different results, as will be shown.

Table 3. Design values for example heavy lift tiltrotors.

Design Value	LCTR	MHTR
Gross weight, lb	124,000	131,000
Rotor radius, ft	44.3	37.5
Number of blades	4	4
Rotor solidity	0.0881	0.0890
Disk loading, lb/ft^2	10.0	14.8
Tip speed, hover, ft/sec	650	750
Tip speed, cruise, ft/sec	350	626
Cruise speed, knots	350	300
Cruise altitude, ft	30,000	4000 (95 F)
Hover altitude, ft	5000 (77 F)	4000 (95 F)
Length, ft	110	98
Wing span, ft	105	89
Wing area, ft^2	1545	1308
Wing loading, lb/ft^2	82	100
Drag D/q, ft^2	37.3	48.3
Engine power, shp	4×6914	2×16454

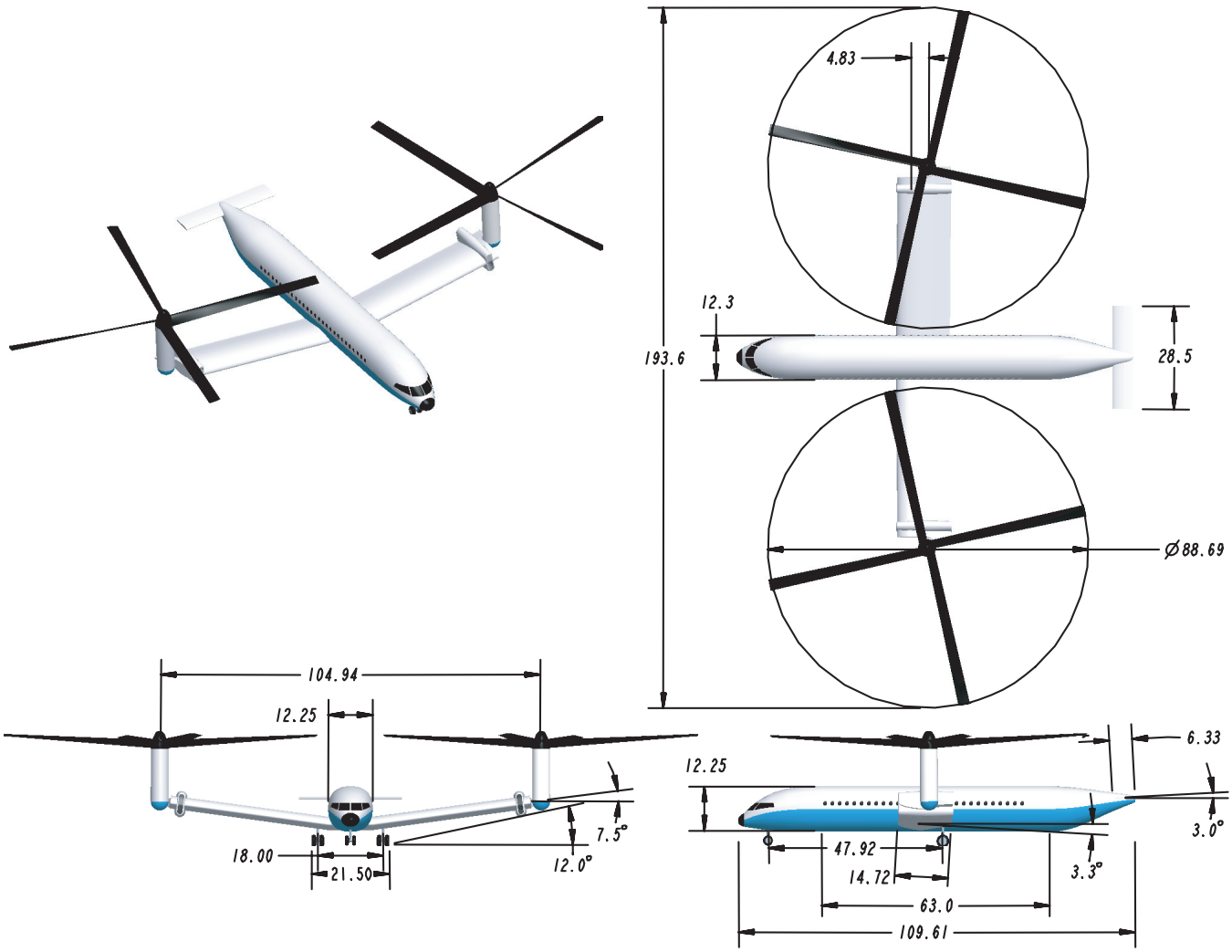

Figure 2. LCTR concept design.

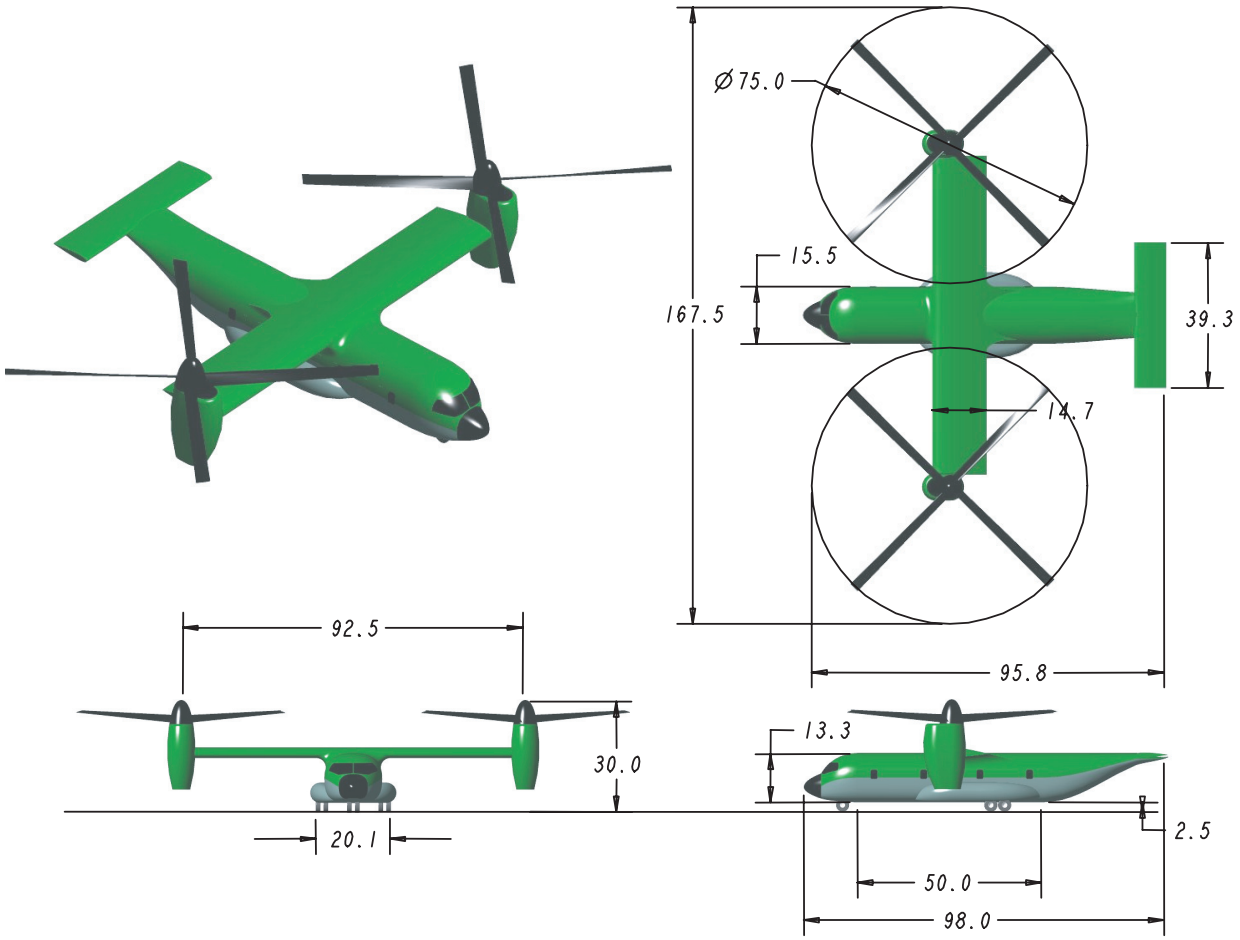

Figure 3. MHTR concept design.

Airfoil design

The airfoil design package HeliFoil is written in a new programming language, PHP-GTK. HeliFoil links the following codes to achieve comprehensive airfoil design, optimization and analysis:

MSES v3.0 for transonic airfoil analysis
LINDOP multi-point design optimizer
Eppler PROFIL98 for conformal mapping airfoil design

The general principles of the airfoil design method are described in Ref. 7.

During the initial pass through the design process, CAMRAD II computed the airfoil operating environment that drove the rotor airfoil design and produced initial estimates of twist and taper. Figures 4 and 5 present the angle of attack vs. Mach number curves for the two aircraft at the design hover and cruise conditions. The figures show the absolute angle of attack, uncorrected for zero-lift offsets. Zero-lift angle of attack was negative for all airfoils, resulting in positive thrust in cruise.

Note that the MHTR rotor has a much broader operating range of angle of attack than the LCTR. Also, the MHTR has considerable overlap in hover and cruise local Mach number, whereas the LCTR has no overlap.

CAMRAD II reads in airfoil section characteristics from external tables, which were generated for the MHTR and LCTR airfoils with MSES. For the LCTR, three sets of airfoil tables were generated: one at the nominal Reynolds number for each airfoil, and two, paired sets matched to hover and cruise Reynolds numbers. Only one set of MHTR airfoil tables was generated, because that aircraft is optimized for both hover and cruise at 4K/95. Comparisons of different approaches to Reynolds number corrections are given for the LCTR, later in this paper.

Table 4 summarizes the target design conditions for the MHTR and LCTR rotor airfoils. In addition to the data in the table, the MHTR blade had a linear transition section between 0.55 and 0.63 R Figures 6 and 7 show the airfoil profiles. Each airfoil was designed to operate over a range of radial locations in both hover and cruise. As a result, there are four design points shown for each airfoil, with two for hover and two for cruise. In addition, the target pitching moment constraint is shown for each airfoil. The tailored pitching moment distribution uses a strategy of cambered inboard airfoils offset by reflexed outboard airfoils. This is

the opposite strategy used for helicopter designs owing to the high twist of tiltrotors. These points show an approximate boundary of the airfoil performance compromise between hover and cruise over the specified range of radial stations.

For a production rotor, some blending will be required, but since each airfoil is designed to work at the endpoints of its radial extent, the blended airfoils should have an increased chance of maintaining good performance. The technique of blending airfoils for heavy lift rotorcraft remains as a topic of future research.

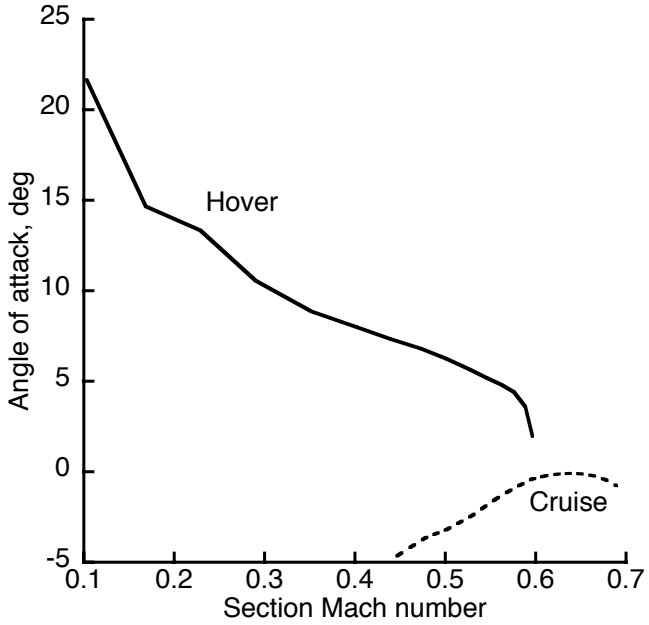

Fig. 4. MHTR rotor airfoil environment.

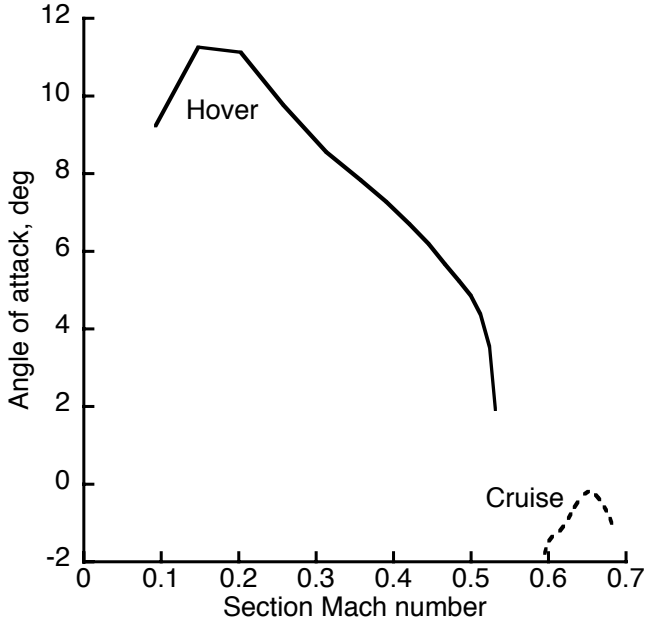

Fig. 5. LCTR rotor airfoil environment.

MHTR Airfoil Design

The challenge for the MHTR rotor airfoil design was to achieve a balance between high lift inboard in hover and low drag at high Mach number across the entire span in cruise. The inboard, high lift airfoil is used to offload the outer working section lift, thereby reducing, for the outer sections, profile drag rise caused by the combination of high subsonic Mach number and moderate lift coefficients. This enables the outer blade section airfoils to operate near maximum L/D at Mach = 0.55 to 0.65, and is the mechanism by which the rotor design achieves higher figure of merit in hover. Without loading up the inboard blade section, the working section airfoils would have been required to operate at lift coefficients beyond maximum L/D and near stall. The reason for this is that stall occurs at relatively low C_l for Mach numbers in the range of 0.55 to 0.65. In contrast, the root section of the blade operates at relatively low Mach numbers, where high C_l can be achieved, especially when root stall delay is considered. The target maximum C_l for the root section is 2.0; however, the airfoil is also required to have low drag in cruise at negative angles of attack.

The resulting airfoil, AFDD HTR1555, meets these constraints by using an aft-loaded design and a special leading edge thickness distribution. The penalty, however, is a large pitching moment, which is offset by using reflexed airfoils outboard to reduce the integrated control loads at the blade root. The C_m constraint on the outer airfoils is made easier to meet by designing the root section for high lift. The working section airfoil provides the most positive C_m contribution, while the tip section requires a near-zero C_m to avoid compromising either hover or cruise performance. In all cases the MHTR airfoils are assumed fully turbulent with transition forced at 2% upper and 4% lower to bracket the movement of the stagnation point.

LCTR Airfoil Design

The challenge for the LCTR rotor airfoil design was very different than for the MHTR, primarily owing to the higher cruise altitude; however, the design strategy was the same. The 30,000ft cruise altitude (compared to 5000 ft for the MHTR) resulted in much higher inboard Mach numbers in cruise. This was especially problematic for achieving high lift root sections without suffering wave drag in cruise from excessive thickness, or in some cases, shock boundary layer separation. As a result, the set of airfoils for the LCTR ended up much thinner, and less reflex could be used over the working section. The root section again used an aft-loaded design with a special leading edge that achieves high lift while preventing supersonic flow in cruise. The outer blade sections were a difficult compromise between preventing supersonic flow (and the associated wave drag and shock boundary layer separation) and achieving high L/D in hover for optimum figure of merit.

Table 4. Tiltrotor airfoil design conditions.

MHTR		Hover (4K/95)				Cruise (4K/95)			
Section	C_m	r/R	C_l	M	Re	r/R	C_l	M	Re
HTR1555	-0.140	0.15	2.00	0.10	1.90×10^6	0.15	-0.66	0.45	8.30×10^6
		0.55	0.80	0.35	6.00×10^6	0.55	-0.30	0.52	8.63×10^6
HTR6383	+0.050	0.75	1.10	0.47	7.10×10^6	0.63	-0.17	0.56	8.80×10^6
		0.83	0.60	0.53	7.71×10^6	0.83	0.30	0.63	9.21×10^6
HTR8399	0.000	0.83	0.60	0.53	7.71×10^6	0.895	0.38	0.64	9.32×10^6
		0.99	0.23	0.59	8.17×10^6	0.99	0.00	0.69	9.47×10^6
LCTR		Hover (5K/77)				Cruise (30K/std)			
Section	C_m	r/R	C_l	M	Re	r/R	C_l	M	Re
CTR1544	-0.160	0.15	2.00	0.09	1.86×10^6	0.15	0.08	0.60	6.00×10^6
		0.45	1.28	0.26	4.90×10^6	0.45	0.16	0.61	5.80×10^6
CTR4475	+0.027	0.45	1.28	0.26	4.90×10^6	0.45	0.16	0.61	5.80×10^6
		0.75	0.96	0.42	7.40×10^6	0.75	0.21	0.65	5.70×10^6
CTR7500	+0.014	0.75	0.96	0.42	7.40×10^6	0.75	0.21	0.65	5.70×10^6
		0.99	0.41	0.53	8.80×10^6	0.99	0.05	0.68	5.70×10^6

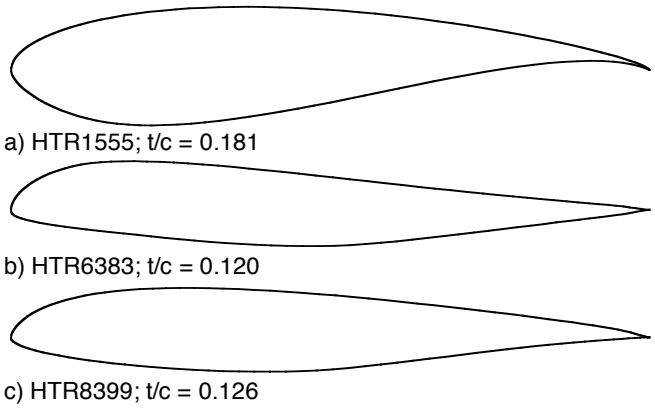

Fig. 6. MHTR rotor airfoils.

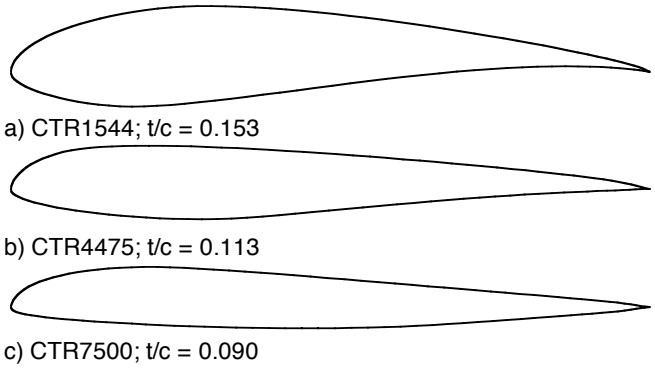

Fig. 7. LCTR airfoils.

In the case of the LCTR, the role of transition was found to be a critical design driver. For these airfoils, transition was assumed to occur at 15% chord on both upper and lower surface, unless it was predicted to occur earlier. This assumption (based on past tiltrotor experience), and the role of transition in heavy lift rotorcraft performance is one of the most critical areas of future work.

Twist and taper optimization

With the newly designed airfoils in hand, the rotors for each tiltrotor were optimized by varying twist and taper and analyzing the resulting performance in hover and cruise with CAMRAD II. Bi-linear twist was used for both rotors: one linear twist rate was applied from the blade root to 50% radius, and a different linear twist was applied from 50% radius to the tip. For each rotor, a large matrix of combinations of inboard and outboard twist rates was analyzed to map out the design space. A nominal value of blade taper, determined by RC, was used for each twist map, then taper was systematically varied for the optimum twist combination. In principle, the aerodynamic twist optimization could be repeated with a new value of taper until twist and taper were both optimized. However, taper was constrained by structural considerations, so further optimization would have not been productive at this stage of the research. Hover figure of merit (M) and cruise propulsive efficiency (η) were chosen as metrics to drive the optimization and to illustrate the results.

MHTR twist optimization

Figure 8 is the twist optimization map for the MHTR, based on an assumed taper ratio of 0.7 (tip/root chord) and using the purpose-designed AFDD airfoils. The rotor was trimmed in thrust to match weight in hover and drag in cruise (Table 3). A free wake model was used for all optimization analyses. The calculations were trimmed to hover $C_T/\sigma = 0.1654$ and cruise $C_T/\sigma = 0.0249$. The optimum twist lies somewhere along the boundary of the map, between the peak value of η and the maximum value of M. Determination of the optimum value is discussed in the section entitled Efficiency Metric, below.

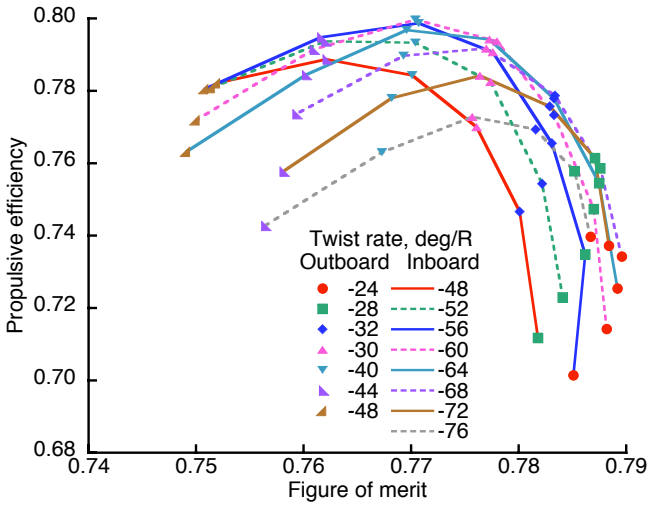

Figure 8. Twist optimization map for MHTR.

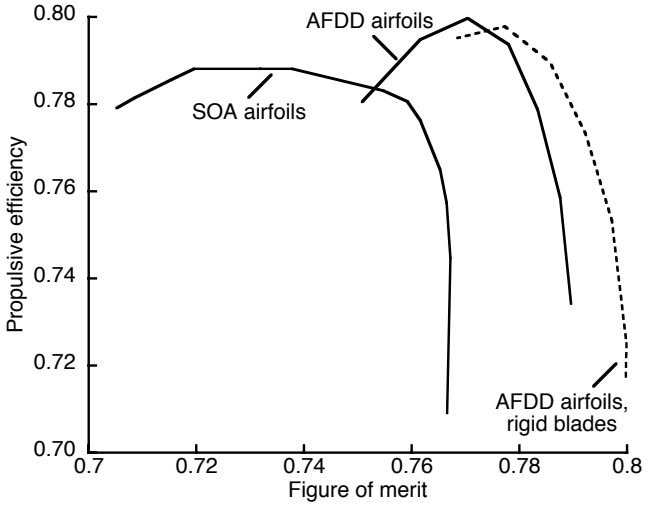

Fig. 9. MHTR twist optimization boundaries for SOA airfoils, AFDD airfoils, and AFDD airfoils with rigid blades.

Figure 9 shows the boundaries of twist maps for AFDD and SOA airfoils. The SOA airfoils were limited to 18% maximum t/c, to avoid excessive inboard drag. The new airfoils yielded a performance improvement of roughly 0.02 M and 0.01 η. This should not be interpreted as indicating any deficiencies in the SOA airfoils, because they were designed for different operating conditions (Ref. 5). Nevertheless, newly designed airfoils should provide substantial improvements in performance. Keep in mind that for such large aircraft, even tiny efficiency improvements can amount to significant improvements in payload or range.

The optimization was repeated with AFDD airfoils and rigid blades, yielding a further improvement in M but a negligible change in η (Fig. 9). With relatively light blades, there is less centrifugal force, hence more coning in hover. The inboard tilt of the thrust vector may be small, but the loss is important. Without blade flexibility, there is no elastic coning and no lift loss. The exact magnitude of loss will of course depend upon the design value of precone. Stiffer blades would increase weight and loads, the penalties of which would have to be traded against the performance gains. This would require further iterations of the rotor design (Fig. 1), well beyond the scope of the present effort.

Efficiency metric

For any given airfoil family, the optimum twist lies along the twist-map boundary (Fig. 9); the exact location depends upon the weighting of hover versus cruise, as determined by the mission specifications. Ideally, all twist combinations along the boundary would be fed back through the full design optimization process (Fig. 1), in order to apply the full mission model in RC and to re-size the aircraft to take full advantage of any performance improvements (or to compensate for shortfalls). However, that would result in every point representing a different aircraft, making direct comparisons impossible.

To better illustrate the principle, and to narrow the range of values to be further analyzed as the design is refined, a simple efficiency metric was devised. It is simply the fuel consumed during the nominal mission (Table 1):

F_c = power x SFC x time on condition (hover + cruise)

This linear model was reasonable for the MHTR, because the mission was specified at constant altitude. A further simplification was to assume constant SFC at each condition, hover and cruise. The mission fuel ratio is the total relative to the best case, and is plotted against figure of merit in Fig. 10. The plot scaling forces the optimum twist combination to occur at unity fuel ratio. The heavy mission weighting toward cruise resulted in an optimum combination very close to maximum η. Numerical results are summarized in Table 5. A full-mission, nonlinear optimization will require iteration between RC and CAMRAD II.

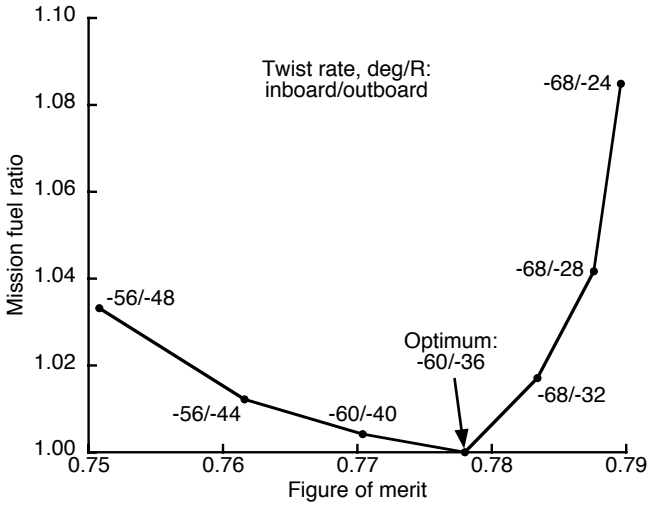

Fig. 10. Mission fuel optimization for MHTR.

Table 5. Twist optimization results for two rotors.

Optimum Value	LCTR	MHTR
Inboard twist, deg/radius	-32	-60
Outboard twist, deg/radius	-30	-36
Taper, tip/root	0.8	0.7
AFDD airfoils:		
Figure of merit	.791	.778
Propulsive efficiency	.828	.794
SOA airfoils:		
Figure of merit	.792	.759
Propulsive efficiency	.806	.781

MHTR taper optimization

A range of taper values was analyzed for the MHTR using the optimum twist combination (Fig. 11). The taper ratio is here defined as the root chord divided by the tip chord. While taper was varied, thrust-weighted solidity was held constant at the value in Table 3 (constant chord at 75% radius).

Pure aerodynamic optimization would suggest zero taper, or even inverse taper. Inverse taper has been proposed by Boeing (Ref. 8) for high speed tiltrotors to reduce root drag. The value chosen here (0.7) was set by blade structural weight. Figure 11 illustrates the penalty of taper without a weight constraint. A higher-order optimization to trade off blade weight against mission fuel burn would require iteration between RC, CAMRAD II, blade structural design, and possibly even airfoil design. Such an ambitious multi-parameter design optimization is well beyond the scope of this paper, but has obvious potential for future research.

Figure 11 also shows the effect of stall delay. Two stall delay models were used, the Corrigan and Selig models, respectively derived from Refs. 9 and 10 (see also Ref. 4). There is little to choose between the two models, largely because they were both calibrated against the same, limited test data. However, without stall delay, there was a significant loss in hover performance over a wide range of taper values.

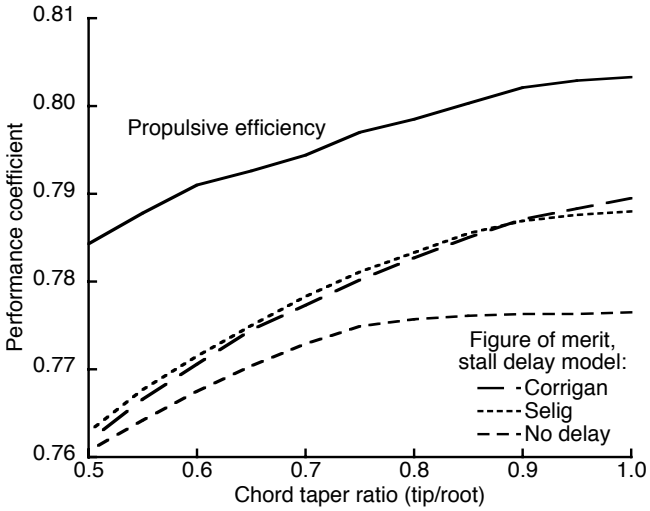

Fig. 11. Taper optimization for MHTR.

LCTR twist optimization

The same twist and taper optimization process used for the MHTR was applied to the LCTR. Figure 12 shows the LCTR twist optimization map. Note the finer variations in twist rate and coefficient scales for LCTR vs. MHTR. This resulted from a higher degree of optimization: the twist range had been narrowed down prior to this optimization run. Also, there was a much lower difference between the inboard and outboard twist rate at the optimum, because of the lower cruise tip speed.

Near the optimum, the difference between the inboard and outboard twist rate was very small, and two different sets of airfoil tables were used, so the performance coefficients (M and η) do not vary smoothly in the plot. The calculations shown in Fig. 12 used a blade taper ratio (tip/root chord) of 0.8, and were trimmed to hover $C_T/\sigma = 0.156$ and cruise $C_T/\sigma = 0.073$. Specifying tighter trim convergence in CAMRAD II would help to smooth out the individual curves, but would make only trivial changes to the optimization maxima, so this option was not pursued.

For the LCTR, the AFDD airfoils are compared to SOA airfoils using two different methods of modeling Reynolds number effects (Fig. 13). CAMRAD II can optionally apply exponential corrections (here, 1/5-power) to maximum lift and drag based on Reynolds number (Ref. 4). The "nominal Re" curves used airfoil tables constructed for a single value of Reynolds number for each airfoil section, then applied the CAMRAD II corrections. The "matched Re" curves were based on airfoil tables generated by MSES specifically for

each operating condition (see Table 4). The CAMRAD II corrections were also applied to the matched tables, but the effect was very small because the local flow conditions were already very close to those assumed in the tables. The "matched Re" properties are preferred because MSES explicitly accounts for Re effects, instead of relying on a correction factor.

For purposes of comparison, a special set of airfoil tables was generated for the SOA airfoils for cruise operating conditions, again using MSES. These tables were generated assuming 15% laminar flow to match the assumptions used for the purpose-designed AFDD airfoils (Table 4).

Figure 13 shows twist optimization maxima for four sets of airfoil tables: the SOA airfoils and the AFDD airfoils, each for both nominal and condition-matched Reynolds numbers. It is evident that Reynolds number had a much greater effect on the predictions than the airfoils themselves. The new airfoils gave an improvement in cruise efficiency of almost 0.01 at the optimum twist combination (Table 5). The new airfoils sacrificed a minor amount of hover efficiency, but only for twist combinations far off the optimum for the LCTR mission.

Blade elasticity caused a more severe loss of figure of merit for the LCTR than for the MHTR; compare Figs. 9 and 14 (but note the expanded scales of Fig. 14). However, blade elasticity resulted in an increase in LCTR propulsive efficiency roughly equal to that provided by the new airfoils. This implies that precone was optimal for neither hover nor cruise. Precone was not optimized for aerodynamic efficiency, but was chosen to reduce hover loads. The tradeoff between blade loads, hence blade weight, and rotor performance has not been studied in any detail for precone, but it adds a new dimension to the optimization strategy that is obviously worth exploring.

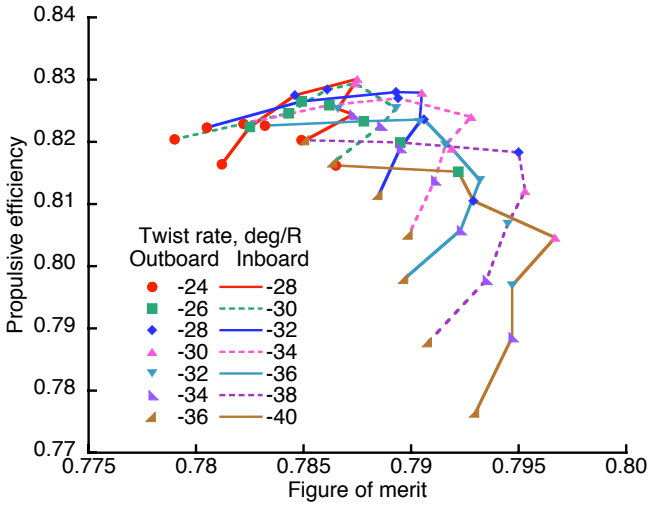

Fig. 12. LCTR twist optimization map for AFDD airfoils. Airfoil tables are matched to Reynolds number.

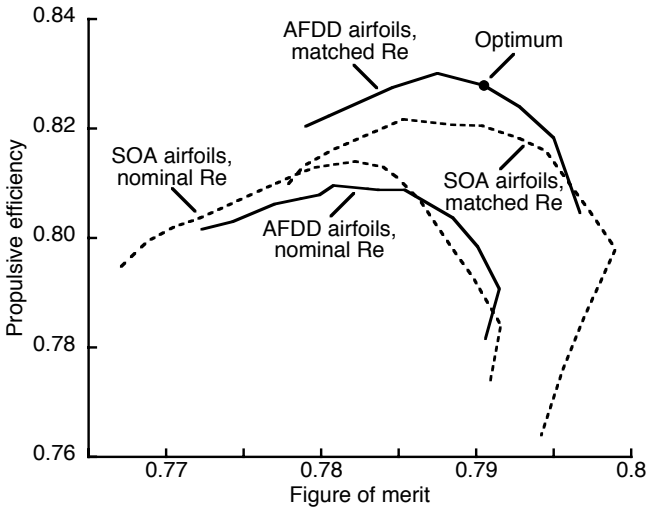

Fig. 13. LCTR twist optimization maxima for two airfoil families, for nominal and condition-matched Reynolds numbers.

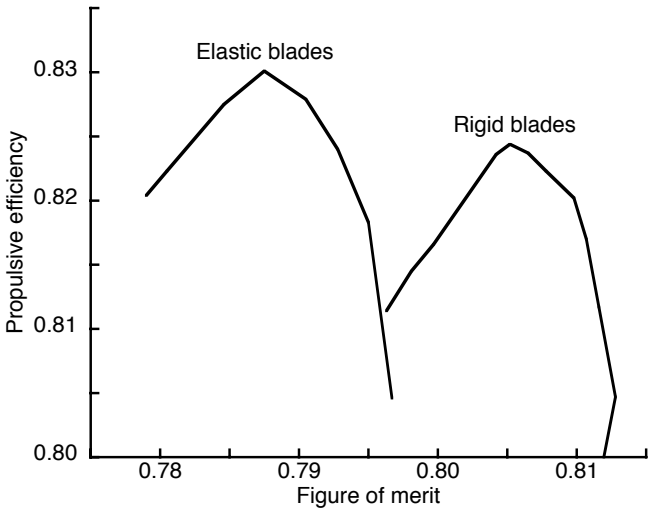

Fig. 14. LCTR performance cost/benefit of blade elasticity.

The LCTR twist-optimization curve for minimum fuel was not a smooth curve. Near the optimum, the difference between the inboard and outboard twist rates was small, and calculations were made for two different altitudes, each with a different set of airfoil tables. A global minimum could be readily found, but the trends were erratic; there was no simple equivalent to Fig. 10. The combination of low disk loading in hover and a heavily cruise-weighted mission placed the optimum twist very close to peak propulsive efficiency (Fig. 13). With the new airfoils, the optimized values of M and η in Table 5 comfortably exceed the values assumed by RC (M = 0.785 and η = 0.812; Ref. 1), whereas the SOA airfoils fall short in η.

It should be emphasized that neither twist optimization plot (Figs. 8 and 12) represents a complete system optimization, and that further performance improvements may be expected from new airfoil designs, especially if pitching moment constraints are relaxed. However, the differences between the two figures are instructive, and may be explained by the different operating conditions of the two rotors. For the LCTR, the low cruise tip speed and the resulting low inboard twist place the blade sections in relatively benign operating conditions. In contrast, the MHTR has much higher cruise tip speed, hence higher optimum inboard twist, which is a much more challenging aerodynamic environment. Therefore, there is more to be gained with new airfoils for the MHTR than for the LCTR.

LCTR taper optimization

Figure 15 shows the taper optimization for the LCTR, given the optimum twist (Table 5). Hover efficiency is weakly sensitive to taper, but cruise efficiency is slightly more sensitive than the MHTR (compare Fig. 11). Stall delay has essentially no effect on taper: such differences as can be detected are attributable to minor variations in CAMRAD II convergence, hence are not shown. This is to be expected: the LCTR has low inboard twist, compared to the MHTR (and to the V-22 and XV-15), so the inboard airfoils are not stalled.

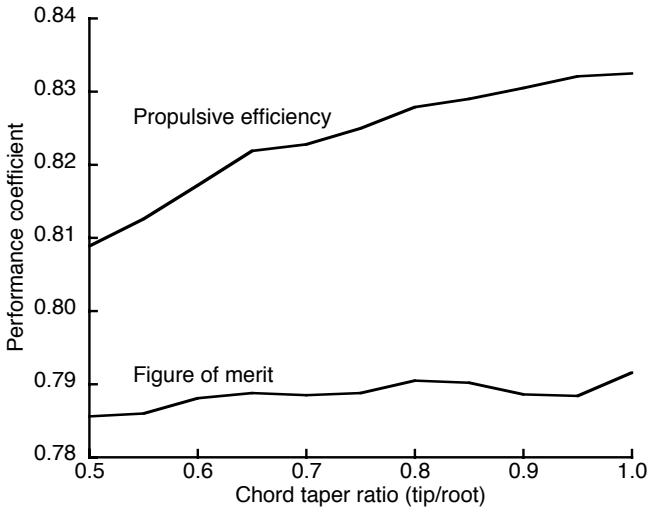

Fig. 15. Taper optimization for LCTR.

A taper ratio of 0.8 was chosen to retain more cruise efficiency than the MHTR. But again, this is not a true system optimum. Taper and airfoil section thickness both affect blade stiffness, so a true optimization of rotor structural weight versus aerodynamic efficiency would require a more complex design process than that of Fig. 1.

Conclusions

Conceptual designs of two very large (130,000-lb class) tiltrotors were developed as part of, and in parallel with, the Heavy Lift Rotorcraft Systems Investigation. A civil design, the Large Civil Tiltrotor (LCTR), was designed to cruise at 350 knots at 30,000 ft; the Military Heavy Tiltrotor (MHTR) was designed to cruise at lower speed and altitude (300 knots, 4K/95). New airfoils were designed for each. The effects of airfoils on the aerodynamic optimization of these two aircraft were studied in some detail, with attention focused on twist optimization and taper to illustrate the effects of Reynolds number, blade elasticity and stall delay.

Compared to current technology airfoils, modern airfoils can provide significant improvement in hover and cruise efficiency at 4K/95 (MHTR). New airfoils can provide slightly less, but still important, improvement in high-altitude, high-speed cruise (LCTR). The differing results for MHTR and LCTR reflect the different mission requirements for the two aircraft.

Reynolds number effects are critical for proper airfoil design and analysis, hence airfoil properties (coefficient tables) must be matched to Re for even minimally accurate estimates of vehicle performance. Refining the assumptions used for transition is an important area of future research.

Rotor flexibility is detrimental to hover efficiency, but can be beneficial to cruise. However, this depends upon precone, which was not optimized for performance. Rotor optimization should be extended to include tradeoffs between aerodynamic performance and rotor weight, including the effects of precone, blade stiffness, and taper. A similar extension to airfoil design would relax pitching moment constraints in return for better performance, and would require trading off aerodynamic efficiency against blade weight and control loads. Such research effort would require higher-order optimization methods than used here.

Acknowledgments

The authors wish to thank Wayne Johnson (NASA Ames Research Center) for his initiative and leadership in developing and sustaining the Heavy Lift Rotorcraft Systems Investigation, and for his invaluable guidance in performing design, optimization and analysis of large tiltrotors. The authors also acknowledge the extremely fruitful synergies engendered by the close cooperation between NASA and AFDD in all manner of rotorcraft research.

References

1. Johnson, W., Yamauchi, G. K., and Watts, M. E., "NASA Heavy Lift Rotorcraft Systems Investigation," NASA TP-2005-213467, September 2005.

2. Yeo, H., and Johnson, W., "Aeromechanics Analysis of a Heavy Lift Slowed-Rotor Compound Helicopter," AHS Vertical Lift Aircraft Design Conference, San Francisco, California, January 2006.

3. Preston, J., and Peyran, R., "Linking a Solid-Modeling Capability with a Conceptual Rotorcraft Sizing Code," American Helicopter Society Vertical Lift Aircraft Design Conference, San Francisco, CA, January 2000.

4. Johnson, W., "CAMRAD II Comprehensive Analytical Model of Rotorcraft Aerodynamics and Dynamics," Johnson Aeronautics, Palo Alto, California, 2005.

5. Narramore, J. C., "Airfoil Design, Test, and Evaluation for the V-22 Tilt Rotor Vehicle," 43rd Annual Forum of the American Helicopter Society, St. Louis, Missouri, May 1987.

6. Zhang, J., and Smith, E. C., "Structural Design and Optimization of Composite Blades for a Low Weight Rotor," 2nd International Basic Research Conference on Rotorcraft Technology, Nanjing, China, November 2005.

7. Martin, P. B., "Rotor Blade Airfoil Design for High-Altitude, Long-Endurance VTOL UAVs," 31st European Rotorcraft Forum, Florence, Italy, September 2005.

8. Liu, J., and McVeigh, M. A., "Design of Swept Blade Rotors for High-Speed Tiltrotor Application," AIAA 91-3147, AIAA, AHS, and ASEE, Aircraft Design Systems and Operations Meeting, Baltimore, Maryland, September 1991.

9. Corrigan, J. J., and Schillings, J.J., "Empirical Model for Stall Delay Due to Rotation," American Helicopter Society Aeromechanics Specialists Conference, San Francisco, California, January 1994.

10. Du, Z., and Selig, M.S., "A 3-D Stall-Delay Model for Horizontal Axis Wind Turbine Performance Prediction," AIAA Paper 98-0021, January 1998.